Simulation of the diurnal variation of rainfall over the western Maritime Continent using a regional climate model

Citation: Im, Eun-Soon and Elfatih A. B. Eltahir. "Simulation of the Diurnal Variation of Rainfall over the Western Maritime Continent Using a Regional Climate Model." Climate Dynamics 51, 1–2 (September 2017): 73–88 © 2017 Springer-Verlag GmbH Germany

As Published: https://doi.org/10.1007/s00382-017-3907-3

Publisher: Springer-Verlag

Persistent URL: http://hdl.handle.net/1721.1/116417

Version: Author's final manuscript: final author's manuscript post peer review, without publisher's formatting or copy editing

Simulation of the diurnal variation of rainfall over the western Maritime Continent using a regional climate model

Eun-Soon Im[1] and Elfatih A. B. Eltahir[2]

[1]Department of Civil and Environmental Engineering/Division of Environment, The Hong Kong University of Science and Technology, Hong Kong

[2]Ralph M. Parsons Laboratory, Massachusetts Institute of Technology, Cambridge, Massachusetts, 02139, USA

[Corresponding author]

Dr. Eun-Soon Im

E-mail: ceim@ust.hk / Tel.: +852 23588190

Address: Academic Building 3594, Hong Kong University of Science and Technology, Clear Water Bay, Kowloon, Hong Kong, China.

Abstract

This study evaluates the performance of the MIT regional climate model (MRCM) in simulating the temporal and spatial structure of the diurnal variation of rainfall over the western Maritime Continent. In order to investigate the effect of model resolution, two identical simulations with 27 km and 12 km horizontal resolutions are performed for a 30-year period (1982-2011). The simulated climatological features are compared with the TRMM 3B42 3-hourly observations. The analysis is focused on the regional characteristics of diurnal variation of rainfall in terms of phase and amplitude, with an emphasis on the difference in behaviors between land and ocean. Systematic modulation of the diurnal cycle over land and ocean characterizes the rainfall pattern over the Maritime Continent. The evening peak with strong amplitude over land and the morning peak with weak amplitude over ocean reflect the contrast in behavior between land and ocean. In general, both simulations are able to capture major features of diurnal rainfall variations with similarity in several aspects to TRMM observation. However, the improvement from increasing resolution is more apparent in the coastal and offshore areas, where rainfall processes are strongly tied with low-level wind that varies diurnally and regionally. A more realistic coastline and a sharp gradient of elevation derived from high resolution boundary conditions enhances the local circulation associated with land-sea breeze and topographic complexity, which in turn induces a favorable condition for the offshore convergence and associated rainfall occurrence. The MRCM with 12 km resolution simulates propagation of rainfall from inland to coastal or offshore areas, such as in the vicinity of western Sumatra, northern Java, and western Borneo Islands. However, further improvements can be gained from even higher resolution models, such as convection-permitting scale.

1. Introduction

Modeling the diurnal variation of rainfall over the Maritime Continent is particularly challenging, potentially leading to substantial errors in simulations of important climate processes including land-atmosphere interaction and diurnal variation of convective heating of the atmosphere. Although the state-of-the-art global or regional models simulate the broad-scale characteristics of mean rainfall reasonably well, their skills in capturing the detailed structure of daily or sub-daily rainfall depend on the regions, seasons, model configurations, and physics parameterizations incorporated into the models. (Sato et al. 2009; Arakawa and Kitoh 2005; Teo et al. 2011; Qian 2008; Wu et al. 2009; Koo and Hong 2010; Birch et al. 2015; Dai et al. 1999; Reboita et al. 2016; Da Rocha et al. 2009). Specifically, it is quite difficult to accurately reproduce the phase and amplitude of the diurnal variation of rainfall in the vicinity of the complex topographical conditions. From the RegCM3 simulations over the Maritime Continent, Gianotti et al. (2012) demonstrated that the results have limited accuracy in reproducing the observed timing of the diurnal rainfall peak irrespective of the choice of lateral boundary conditions, the cumulus parameterizations, and land surface schemes. Love et al. (2011) performed simulations with 40 km and 12 km resolutions over the Maritime Continent using the UK Met Office atmospheric model and demonstrated that the amplitude of the diurnal cycle is weak over the coastal seas and the timing of maximum rainfall over land is too early.

In order to improve the simulation and understanding of important mechanisms that control the diurnal variation of rainfall, two types of approaches have been tried: 1) improving the convective parameterization or resolving it explicitly to reduce the uncertainties or errors from the representation of subgrid-scale processes (e.g., Lee et al. 2008; Sato et al. 2009; Gianotti 2012; Birch et al. 2015; Pritchard and Somerville 2009; Wang et al. 2007; Takayabu and Kimoto 2008) and 2) increasing resolution to better resolve the heterogeneity of complex topography and land-sea contrast (e.g., Lee et al. 2007; Sato et al. 2008; Ploshay and Lau 2010). All these studies demonstrate complexity of diurnal variation of rainfall, this complexity is such that no single parameter brings a dramatic improvement in simulation of diurnal variation. In addition, the sensitivity to diurnal variation of rainfall to model parameters varies across regions and models.

In this study, we investigate the performance of the MIT regional climate model (MRCM, Im et al. 2014) in simulating the rainfall over the Maritime Continent and its sensitivity to horizontal resolution (27 km vs. 12 km). Although MRCM is fundamentally based on the Regional Climate Model version 3 (RegCM3, Pal et al. 2007), the skill of MRCM has been improved through the incorporation of new physics schemes and modification of existing schemes. Most importantly in modeling climate of the Maritime Continent, Gianotti and Eltahir (2014a, b) revised the parameterizations for convective cloud fraction and convective rainfall autoconversion scheme within MRCM. Unlike the old version of RegCM3 with the assumption that cloud fraction is distributed randomly and uniformly in a model grid cell, they adopt the idea that the grid-mean cloud liquid water (CLW, prognostic variable) can be used to infer the area covered by convective cloud. Given that direct linkage between simulated cloud cover and simulated CLW brings the physical realism with respect to the interconnected variations between cloud cover and radiation, they argue that their modification improves the cloud-radiative feedback that could in turn affect the simulation of rainfall in a positive way. Hence, we extend these efforts in the validation of MRCM performance focusing on the diurnal variation of rainfall and expect further improvement from enhancement of the horizontal resolution. In this regard, we emphasize on regional characteristics of diurnal variation of rainfall during wet season (i.e. December-January-February: DFJ) by comparing the results from different resolutions (27 km vs. 10 km) and different regions (land vs. ocean). Improving simulations of the diurnal variation of rainfall does not resolve all the deficiencies in simulations of the water cycle over the Maritime continent. However, since the diurnal variation of rainfall plays a key role in shaping the climate over the Maritime Continent (Gianotti 2012; Oh et al. 2012), any improvement in the skill of MRCM can enhance the reliability of MRCM as a useful tool to produce climate information over this region.

2. Model description and experimental design

2.1. MRCM description

The MIT Regional Climate Model (MRCM) used in this study is based on the Regional Climate Model Version 3 (RegCM3, Pal et al. 2007). MRCM maintains much of the same structure of RegCM3 but with several important improvements, including (1) coupling to the Integrated Biosphere Simulator (IBIS) land surface scheme (Winter et al., 2009); (2) a new bare-soil albedo assignment method (Marcella, 2012); (3) new convective cloud and convective rainfall auto-conversion schemes (Gianotti and Eltahir, 2014a,b), and (4) modified boundary layer height and boundary layer cloud schemes (Gianotti, 2012). Based on the evaluation of MRCM simulations against the original version of RegCM3 or various state-of-the-art regional climate models, MRCM has consistently showed comparable or better performance in simulating key climate features across various regions (e.g., North America, West Africa, Southwest Asia, Maritime Continent). In particular, the version of MRCM that combines IBIS land surface scheme and the modified Emanuel convection scheme incorporating the new convective cloud cover and new convective rainfall autoconversion improves the cloud-radiative feedback over the Maritime Continent, highlighting the importance of representation of subgrid-scale variability in diurnally varying convective processes (Gianotti and Eltahir, 2014a,b). More specifically, the factional area of a model grid cell that is covered by convective cloud is determined by the ratio of simulated grid-average CLW to climatological observed CLW. Autoconversion of convective rainfall is made to be a function of the subgrid variability in simulated CLW, which is constrained by typical observational value of CLW. These new parameterizations bring physical realism in diurnally varying convective processes, compared to the old version with the assumption that the cloud fraction in a grid column is distributed randomly in space between the model layers and clouds fill the grid cell uniformly in the vertical direction. For example, the new parameterizations increase low cloud cover in the early afternoon, concomitant with convective activity, resulting in improved simulation of the diurnal cycle of incoming solar radiation. The new parameterizations also exhibit a distinct diurnal cycle in high large-scale clouds cover, with more cloud generated in the late afternoon and nighttime, which is consistent with observed feature over the Maritime Continent. Therefore, we adopt the same physics parameterizations of MRCM used for Gianotti and Eltahir (2014a,b) with additional calibration (see section 2.2). More detailed model description of MRCM and basic performance can be found in Gianotti and Eltahir (2014a,b), and Im et al. (2014).

2.2. Experimental design and data used

Figure 1 shows the domain focused on this study and topography used for MRCM simulations with 27km and 12km horizontal resolutions, which are denoted as MRCM27 and MRCM12 hereafter. Domain covers the western part of the Maritime. The boundary conditions entail the use of a relaxation and a diffusion term throughout a lateral buffer area, 6 grid points and 12 grid points in MRCM27 and MRCM12, respectively. We have selected this domain following a few sensitivity experiments in terms of domain size. Since a larger domain that extends to further into the ocean area does not bring relevant difference over our target region, we decided to use the domain in Figure 1 considering the computational burden for long-term climate simulation.

Comparison of the topography prescribed by MRCM27 and MRCM12 clearly demonstrates how the representation of topography depends critically on the model resolution. For example, MRCM12 captures the prominent mountainous ranges reaching elevations of 1000 m along the western Sumatra

Island. Wu et al. (2009) highlighted the role of these mountains and the associated thermally and convectively induced local circulations in the formation of nocturnal abundant rainfall over the sea west of Sumatra Island. Therefore, it is reasonable to expect that MRMC12 is more skillful in simulating topographically induced local circulation, with significant impact on the diurnal cycle of convective activity.

The initial and boundary conditions are from the ERAInterim reanalysis with a resolution of 1.5°X1.5° at 6-hour interval (Uppala et al. 2008). The simulations span 30-year and 1-month from December 1981 to December 2011, and the results from the first 1-month are excluded in the analysis as a spin-up period. The sea surface temperatures (SSTs) are prescribed from the National Oceanic and Atmospheric Administration (NOAA) Optimum Interpolation (OI) SST dataset with a horizontal and temporal resolution of 1°X1° and weekly interval, respectively. Since the SSTs at weekly time-scale are temporally interpolated to daily time-scale to provide the time-varying boundary condition, these simulations do not take into account the diurnal variation of SSTs. This assumption may restrict the full dynamics of land-sea circulation in response to SST variation.

Several parameters are customized to optimize the model performance under the current domain setting and initial and boundary conditions that are different from those of Gianotti and Eltahir (2014a,b). Since the specific values used for new parameterization for autoconversion in convective clouds such as climatological cloud liquid water and threshold cloud water content calculated from critical droplet concentration and critical dropt radius are chosen (see Table 1 in Gianotti and Eltahir 2014a). For example, climatological observed CLW has the range of 0.25-1.3 (g m^{-3}), and Gianotti and Eltahir (2014a,b) select CLW=1.2 (g m^{-3}) over land and CLW=0.7 (g m^{-3}) over ocean. Then, the threshold of CLW (CLW_T) is determined for the calculation of the autoconversion efficiency. For this, Gianotti and Eltahir (2014a,b) assign CLW_T=1.5 (g m^{-3}) over land and CLW_T =0.7 (g m^{-3}). We adjust these parameters from within ranges of observed values based on sensitivity tests for our domain configuration as indicated by Table 1.

For comparison to the rainfall derived from MRCM27 and MRCM12 simulations, Tropical Rainfall Measuring Mission (TRMM) 3B42 product with 3-hourly temporal and 0.25°X0.25°spatial resolution is used (Huffman et al. 2007). TRMM 3B42 product is used for the validation of MRCM performance for both monthly and diurnal time-scale. Note that TRMM observation is not available during the same period of simulations. Hereafter, 14-year (1998-2011) climatological features derived from TRMM-3B42 are simply denoted as TRMM, whereas both simulations are based on the 30-year (1982-2011) climatology.

3. Results

3.1. Regional characteristics of mean rainfall

We begin our analysis of the climatological aspects of rainfall by focusing on simulations of general characteristics over the Maritime Continent. Figure 2 presents the spatial distribution of wet-season (December-January-February: DJF) mean rainfall derived from MRCM27 and MRCM12 simulations, and TRMM observations, and difference between simulation and observation. In the boreal winter season (DJF), there is more rainfall over this region than in the boreal summer season (June-July-August: JJA). In spite of the general similarity in qualitative aspects of rainfall distribution, the model deficiencies are clearly revealed in the bias patterns against TRMM observation. The dominant patterns appearing in both MRCM27 and MRCM12 simulations are unrealistic excessive rainfall along the high mountainous region and the systematic underestimation of rainfall over the ocean. Strong positive bias along the mountain range is not a unique feature in our simulations. Rather, this bias is consistently exhibited in many other simulations. For example, Da Rocha et al. (2009) showed that RegCM3 tends to simulate excessive rainfall over the eastern side of the Andes and western Peru characterized by high topography. They pointed out possible reasons for excessive rainfall including intense orographic uplift and some numerical errors in sigma vertical coordinates system. On the other hand, Xu et al. (2006) reported a systematic error in summer rainfall along a mountainous region such as the edge of the Tibetan Plateau using PRECIS regional climate model, highlighting the over-sensitivity of parameterization of rainfall processes to topography. Alternatively, this error can partly be due to observational undersampling where short-lived intensive rainfall could have been missed by the 3-hourly sampling period of 3B42 TRMM observation (Teo et al. 2011). In contrast to systematically overestimated rainfall along the mountainous region, severe dry biases prevail across most of the ocean, particularly in MRCM27 simulation. The positive impact of higher resolution appears in the simulation of rainfall over the ocean. MRCM12 shows relevant reduction of dry bias seen in MRCM27 simulation, hence bring improvement in DJF rainfall in both its quantitative and qualitative aspects. Specifically, MRCM12 and TRMM similarly show intense rainfall over the sea adjacent to the coast of the northwestern Borneo Island, sea off the western coast of Sumatra Island, and northern coast of Java Island. Such intense rainfall in the vicinity of the coastal or offshore areas is a dominant feature observed in TRMM, but is absent in MRCM27. Interestingly, this improvement of MRCM12 is quite in line with the results from Love et al. (2011), using an entirely different model. They conclude that the 12 km resolution shows a substantial improvement in the simulation of the oceanic rainfall of the Maritime Continent that is underestimated in their 40 km resolution simulations.

Modeled characteristics in annual (ANN) and dry season (JJA) mean rainfall are not much different from those during wet season (DJF). Table 2 presents such behaviors in a quantitative manner. Regardless of the season, mean rainfall consistently overestimates (underestimates) observations over land (ocean). However, MRCM12 tends to reduce severe dry bias over the ocean, leading to general improvement over the whole domain. Despite persistent bias, both MRCM12 and MRCM27 simulations reasonably capture the seasonal variation of rainfall, reproducing wetter conditions in DJF and drier conditions in JJA.

To investigate the north-south propagation of rainfall, we present the latitude-time cross-section of the zonally-averaged (95-119°E) monthly rainfall (Fig. 3). MRCM12 consistently shows improvement not only in magnitude but also in the shape of the evolutionary pattern, including realistic positioning of the intense rain band during the wet season. While MRCM27 shows a discontinuity in the evolution of rainfall, which exceeds 9 mm/day, MRCM12 simulates an intense rain band across whole latitudinal extent, which is much closer to observed pattern. This improvement is mainly due to an increase in oceanic rainfall. In addition, MRCM12 simulation successfully captures the high intensity rainfall more than 11 mm/day, extending up to 4°S during the wet season. A similar behaviour can be also found in the longitude-time cross-section of the meridionally-averaged (8°S-7°N) monthly rainfall (not shown).

In summary, MRCM shows reasonable performances in capturing key features of rainfall climatology over the Maritime Continent. Generally, both MRCM12 and MRCM27, with different resolutions (12km vs. 27km), simulate the mean seasonal variation and corresponding spatial pattern of rainfall reasonably compared to observed pattern. However, MRCM12 tends to reduce the severe dry bias over ocean and coastal regions, improving the accuracy in simulation compared to MRCM27. Based on the cross-sectional pattern for latitudinal migration, higher resolution also brings positive effects to the simulation in terms of placement of intense rainfall zones and evolutionary pattern of the rainfall field. In the next section, we focus analysis for diurnal variation of rainfall during DJF which is wet season.

3.2. Rainfall diurnal variation and related circulation pattern

Here, we focus on the phase and amplitude of the diurnal cycle of the rainfall over the Maritime Continent. Both the model and observed data are arranged in coordinated universal time (UTC) with 3hour interval, but we also provide the local solar time (LST) in the center of the model domain. We directly examine the 3-hourly data of rainfall to estimate its diurnal variation, rather than fit the data with multiple harmonics because diurnal variations of rainfall are quite different from simple harmonics (Dai et al. 1999). In assessing how well the simulated peak timing in the diurnal variation match with the one from TRMM observation, raw rainfall simulations from MRCM27 and MRCM12 are first spatially interpolated into the same grid of TRMM observation. DJF mean diurnal variations are then calculated. Otherwise, all analyses are performed based on their own grid system of MRCM27 and MRCM12 simulations, or TRMM observation.

First, in order to provide a quantitative measure of general contrast of the diurnal cycle over land and ocean, we separately present the diurnal variation of rainfall averaged over land and ocean (Fig. 4). As demonstrated in previous studies (e.g., Mori et al. 2004; Ichikama and Yasunari 2008; Wang et al. 2007), there is a distinct difference in diurnal variation of rainfall between land and ocean. The TRMM observed pattern shows a roughly out-of-phase diurnal variation over land and ocean. While the maximum rainfall averaged over land is at 19LST, the same peak is located at 07LST over the ocean. In addition to difference in phase, the amplitude of diurnal variation behaves differently. Rainfall averaged over land shows a stronger variation than over the ocean. Compared to TRMM observed pattern, both simulations show a reasonable performance in capturing major characteristics of diurnal variation between the land and ocean. However, there are several systematic errors in the simulations, and the magnitude of the error depends on horizontal resolution. The most notable deficiency in both simulations is the phase shift of rainfall over the land. The model peaks about three hours earlier than in the TRMM observations. This is a rather typical error for most other regional and global models (Zhou and Wang 2006). After peaking at 16LST, MRCM shows a sharp drop in the rainfall intensity at 19LST. MRCM behaves differently from TRMM observation maintaining its peak for a longer period. In addition to phase shift, the MRCM exhibits higher rates in both maximum and minimum peaks. In general, MRCM12 and MRCM27 manifest similar shapes of diurnal variation, thus presenting the same problem. However, MRCM12 shows slightly better performance, closer to TRMM during the period from 19LST to 01LST. Moving to the ocean area, MRCM reasonably captures the minimum peak at 19LST, however, both simulations systematically underestimate the rainfall rates.

The impact of high resolution tends to be more prominent over the ocean. MRCM12 reduces a severe dry bias, producing more rainfall throughout the entire daily cycle, closer to TRMM than MRCM27 simulation. Nevertheless, the difference between MRCM12 and TRMM are statistically significant except for 19LST and 22LST at the 95% confidence level based on a two-tailed Student's t-test. In terms of interannual variability, MRCM12 shows a mixed performance, reducing variability range over land but enhancing it over ocean compared to those from MRCM27. Despite this limited accuracy, the performance of MRCM12 shows a significant improvement compared to previous versions of the same model (Gianotti et al. 2012; Gianotti 2012).

In the following, we focus on the detailed regional characteristics. Figure 5 presents the spatial distribution of timing of maximum rainfall from both simulations and TRMM observation. Consistent with remarkable contrasts seen in area-averaged patterns, there are distinct regional differences between the land and ocean. While the maximum rainfall over the ocean mostly appears at 04LST, 07LST, and 10LST (blue and dark blue), rainfall peaks at 16LST to 22LST (yellow and green) are dominant over land. In general, a rainfall peak develops in the afternoon and evening over the inland area, and subsequently propagates to the coastline and the ocean. Overall, the model results are in good agreement with these characteristics obtained from TRMM observation, but substantial discrepancies exist in some regions, indicating that the model performance varies from region to region. The most relevant problem appears across a large flat area in Borneo Island, and increasing resolution does not bring the improvement. There is a big mismatch in phase, leading to peaks about three to twelve hours earlier than TRMM. A large mismatch in Borneo Island occurs because the simulation fails to capture the delayed peaks associated with the convective response of the lower atmosphere to shortwave radiative heating (Gianotti 2012). In addition, Wang et al. (2007) demonstrated that the enhancement of the fractional convective entrainment/detrainment rate could prolong the development of deep convection and delay the time of the rainfall peak, thus improving the simulation of rainfall diurnal cycle to some degree.

On the other hand, the impact of higher resolution is clearly revealed in the coastal and off-shore regions associated with the propagation of the rainfall peak. To facilitate this comparison, a close-up look of one representative region over Sumatera Island (see red rectangular box in Fig. 5) is presented in Fig. 6. Sumatera Island has received much attention due to migration pattern of diurnal rainfall peak away from the southwestern coastline of Sumatera Island (Mori et el. 2004; Wu et al. 2009). For the southwestern part of Sumatera Island, the mountainous range (dashed line in Fig. 6) tends to bifurcate the peak time of rainfall. Once rainfall peak occurs predominantly along the mountainous area in the afternoon (16LST, yellow color), this peak propagates both sides toward further inland (northeast) and coast area (southwest). An important point is that the model performance in simulating this propagating feature depends on resolution. More specifically, MRCM12 presents the transition time band where rainfall peaks at 22LST and 01LST along the sea in the vicinity of the coastal region even though its width is narrow compared to TRMM observation. In contrast, MRCM27 poorly simulates this feature, showing much larger phase shift compared to MRCM12 over this region. A significant difference between MRCM12 and MRCM27 is also found in the further inland propagation from mountainous range. Therefore, the impact of horizontal resolution on the simulation of diurnal phase of rainfall does not seem consistent with the geographical location, with the improvement of MRCM12 over MRCM27 varying from region to region. For example, while the resolution impact seems to be marginal across the relatively flat area of the Borneo Island, the impact of resolution is significant in the vicinity of the sea next to Sumatra Island where high mountains with more than 1000 m elevation are located close to its western coast.

In order to demonstrate qualitatively how well simulated peak timing matches with the one from TRMM observation, we calculate fractional areas where the simulated peak timing in the diurnal variation corresponds either exactly to the one from TRMM observation (0 Hour) or is delayed/ advanced within 3hour compared to the one from TRMM observation (±3 Hour) (Table 3). In case of the exact coincidence between the simulation and TRMM observation, MRCM12 consistently shows higher fraction in both land and ocean. However, when we extend criteria up to ±3 hours gap, MRCM12 and MRCM27 show similar results in ocean. Since ocean coverage is huge including vast areas away from the coast, it is difficult for MRCM12 simulation to make significant difference based on the improvement in relatively small limited area along the coast.

Next, in order to investigate the behavior of the normalized amplitude in diurnal variation, we present the spatial distribution of rainfall difference between maximum and minimum phase in the diurnal cycle normalized by daily mean rainfall at individual grids (Fig. 7). First, errors seen in DJF mean rainfall pattern directly feed into this normalize amplitude over the land. For example, strong positive biases along the western Sumatra lead to lower amplitude due to its normalization by mean value. On contrary, negative biases in the eastern plain parts of Sumatra derive relatively higher amplitude due to the same reason. Moving to the ocean, the severe underestimation of rainfall rates corresponding to maximum phase (see Fig. 4 (b)) retains lower amplitude over the sea, in spite of normalized by lower mean value.

Both MRCM12 and MRCM27 show a similar problem over the ocean, but the amplitude of the diurnal cycle of rainfall tends to be enhanced with increasing resolution. In particular, the enhancement along the off-shore near coastal regions is significant, which is mostly due to the enhanced rain rates at the maximum phase (see Fig. 4 (b)). Both simulations show the limited performance in simulating the diurnal variation of rainfall in terms of the maximum phase and normalized amplitude over the south-central part of Borneo Island, regardless of the horizontal resolution.

In order to investigate the relative role of convective and large-scale rainfall in determining the total rainfall pattern in response to increasing resolution, we present the time-longitude cross section (horizontal dashed line along 3°S in Fig. 1) of total, convective, and large-scale rainfall derived from MRCM27 and MRCM12 simulations (Fig. 8). First, the cross-sectional convective and large-scale rainfall show substantial differences in their diurnal variations, which seems to be strongly tied to the geographical distribution of the land and ocean. While the total rainfall is almost entirely contributed by convective rainfall in the afternoon to evening over land, both convective and large-scale rainfall contribute in the morning and nighttime over sea in the vicinity of coastal region. Predominantly convective rainfall in the peak phase over land is consistent with the analysis of TRMM satellite Precipitation Radar (Mori et al. 2004; Ichikawa and Yasunari 2006).

Enhancement of rainfall with increasing resolution over ocean is mainly due to the large-scale rainfall rather than convective rainfall. Indeed, convective rainfall depends little on the horizontal resolution, showing a great similarity between MRCM12 and MRCM27. On the other hand, MRCM12 produces much more large-scale rainfall than MRCM27 from the coastal land to off-shore in the adjacent sea. In particular, propagation of rainfall toward the sea from coastal land is discernible in the large-scale rainfall simulated by MRCM12. For example, the westward propagation (Fig. 8(f)) of large-scale rainfall starting around 15UTC is an important feature, which is absent from MRCM27 simulation.

Therefore, this result suggests that better representation of topography and land-sea contrast can improve the simulated characteristics of large-scale rainfall, due to explicitly resolved processes. The different behavior seen in large-scale rainfall results in different performance in total rainfall derived from MRCM27 and MRCM12 simulations. By comparison with MRCM27, MRCM12 is in better agreement with TRMM observation (Fig. 8(g)) in terms of propagation feature in ocean.

The differences in rainfall diurnal variation between land and ocean reflects the key mechanisms that modulate differences in rainfall characteristics between land and ocean, such as land-sea breeze. Many previous studies have consistently demonstrated the strong influence of the local circulation induced by topography (e.g., ridge and valley) and land-sea contrast on the rainfall diurnal variation. In this regard, we first consider low-level dynamics as the possible reason that MRCM12 shows the better representation of diurnal variation of rainfall along the coastal and offshore region. Figure 9 presents the spatial distribution of anomalous wind and divergence at 925 hPa at 19LST and 07LST. Anomalous winds at each time (e.g., 19LST, 07LST) are computed by subtracting daily mean value. Regardless of resolution, wind directions are apparently reversed in accordance with the sea-land breeze circulation. Particularly, these circulations dominate along the western Sumatra and northern Java where strong migration of rainfall occurs in the offshore coastal region. By the late afternoon and evening (e.g., 19LST), the sea breeze penetrates inland and resultant low-level convergence enhances the rainfall over the mountainous region. However, the low-level dynamical conditions change in the exact opposite direction after midnight to early morning (07LST). The development of strong land breeze results in divergence along the mountain but convergence in the offshore coastal region. This feature contributes to the offshore propagation of rainfall in the morning. Both MRCM12 and MRCM27 show a low-level circulation of generally similar patterns, but with different magnitude. Not surprisingly, the sharp gradient of orographical forcing in the higher resolution simulation can lead to the stronger convergence or divergence, which in turn controls the intensity of local circulation. For example, MRCM12 forms stronger and wider convergence zone in the vicinity of coastline than that of MRCM27 because of the different intensity of topographically-forced motions. Different slopes, along ridges and valleys, directly affect gradients of radiative heating and cooling rates and the intensity of upslope and downslope winds (Liu et al. 2009; Zhou and Wang 2006). Since topographic heterogeneity in fine-scale grid is characterized by more realistic grid-averaged elevation as well as the standard deviation of elevation, higher resolution allows for larger slopes, which would be reflected in higher gradients of radiative heating/cooling and related thermodynamic processes, likely forcing stronger circulation.

This different behavior in accordance with different resolution can be seen more clearly in the vertical cross section. Figures 10 presents the distribution of omega and vertical circulation along the terrain transects. First, the reversal of sea and land breeze and related circulation patterns within a 12 hour interval are evident in both simulations. However, important differences exist in the details related to the topographical modulation of the vertical motion. In the evening (e.g., 19LST), MRCM12 shows much stronger ascending motion over the mountain. More importantly, in the morning (e.g., 07LST) relatively wider extent of ascending motion (farther south of 4°S) simulated in MRCM12 is a result of stronger descending motion along the downslope associated with the radiative cooling in the night time and early morning. Such behaviors are more pronounced in response to the complex terrain. In addition to the lower height of mountain peak, the topography prescribed in MRCM27 does not resolve the fluctuating features consisting of ridges and valleys that are evident in the north-south transects of MRCM12. Vertical motion seems to be constrained by topographical modulation, demonstrating the importance of a refined surface forcing for improving the accuracy of local circulation. This finding is in line with results using the different models, such as global cloud resolving model (Sato et al. 2009) and International Pacific Research Center regional climate model (Zhou and Wang, 2006). All these simulations support the conclusion that topography plays a critical role in simulations of the diurnally-varying thermal circulation, and the associated diurnal variation of rainfall.

4. Summary and Discussion

This study aims at evaluating the MRCM performance in simulating the rainfall characteristics over the western Maritime Continent and at assessing the potential of this regional climate model with higher resolution to better resolve complex climatic processes that are mainly regulated by geographical characteristics (e.g. land-sea contrast, topography). In particular, we place our emphasis on the diurnal variation of rainfall and related regional-to-local circulations. For this, the two simulations with different resolutions of 27 km and 12 km are performed for a 30-year period, with all other conditions being identical. Comparison of MRCM with different resolutions (27 km vs. 12 km) shows that a higher resolution has improved performance in simulating the migrating patterns of rainfall in the vicinity of offshore along western Sumatra and northern Java, two regions characterized by sharp gradients and complex topography. However, the improvement by higher resolution is not consistent across the whole domain, indicating the regional dependency. For example, the diurnal variations of rainfall simulated by MRCM12 and MRCM27 do not show relevant differences over the plains in the central regions of the Borneo Island that reveals the large shift of maximum phase in the diurnal variation of rainfall. A similar systematic bias is addressed by the work of Wang et al. (2007), and they demonstrate the positive effect on the correction of the peak phase by enhancing entrainment/detrainment rates in the mass flux convective parameterization scheme using the regional climate model. Therefore, the potential for improvements in simulations of the phase and amplitude of diurnal variation of rainfall seems to be limited if we enhance resolution without improving convective parameterization. On the other hand, Takayabu and Kimoto (2008) point out that their modification of Arakawa-Schubert cumulus parameterization does not improve the phase shift of the rainfall diurnal variation over the Maritime Continent compared to other regions like Central America and West Africa that show large improvements. They attribute the reason to the insufficient resolution of global model (T106, approximately 1.125° × 1.125°) to adequately simulate precipitation over the complicated topography of the Maritime Continent.

The processes regulating the diurnal variation of rainfall are complex and controlled by the interactions of many different factors (e.g., Evans and Westra 2012). In addition, dominant factors are dependent on the regions, such as atmospheric instability and thermal convection over southeastern Australia (Evans and Westra 2012) and vertical differential thermal advection over southeast China (Huang and Chan 2011). Our study emphasizes the impact of horizontal resolution on the diurnal variation of rainfall over the western Maritime continent where the surface boundary conditions are complex. Higher horizontal resolution contributes to better resolving the complex topographical features and surface heterogeneity (e.g., land-sea contrast) (Leung and Qian 2003). In particular, Sumatra, Java, and Borneo islands included in the simulation domain are characterized by topography with sharp gradient and large fluctuations. Such features can immediately affect regional to local circulation patterns through the land-sea and mountain-valley differential heating and orographically forced ascending or descending motion. The gradients of heating/cooling associated with slope is key factor in modulation of the intensity of vertical motion (Liu et al. 2009; Zhou and Wang 2006). The analysis of vertical cross-section of wind and omega along the complex terrain clearly demonstrates that smoothed orography in MRCM27 can not effectively force vertical motion as strong as in MRCM12, subsequently resulting in the weak low-level convergence. The main reason that MRCM12 significantly improves the rainfall migration pattern into the coastal and off-shore regions (e.g., 24UTC) from the mountainous peak (e.g., 12UTC) is explained by the stronger ascending and descending motion. For example, the steeper downslope seems to produce stronger descending motion due to gradients of radiative cooling at night time, which enables strong land breeze enhancing the ascending motion farther in the offshore region. Capturing this enhanced local circulation in higher resolution model plays a role in improving the simulation of rainfall pattern over the coastal and offshore in the morning, bringing them closer to TRMM observed pattern. This is a good illustrative example to show that a high resolution, including a more refined representation of topography, can improve the simulation of the diurnal variation of rainfall, in geographically diverse region like the Maritime Continent. The importance of local land-sea circulation was also highlighted in a study of the diurnal cycle of rainfall in Malaysia using ground-based hourly observations (Oki and Musiake 1994).

It is noted that our conclusion is derived from one particular regional climate model, MRCM. It implicitly indicates the model dependence on our results. In other words, it is rather difficult to generalize the findings that we have emphasized in this study. However, there are relevant literatures to support our study, suggesting the necessity of higher resolution for improving the simulation of the diurnal variation of rainfall using entirely different modeling system. Love et al. (2012) demonstrated using the UK Met Office Unified Model that the simulation with 12 km resolution shows the better performance than that with 40 km resolution in simulating rainfall over the Maritime Continent. Furthermore, the phasing of the diurnal cycle of propagating offshore convection becomes more accurate in the 4km model with explicit convection. Similarly, Sato et al. (2009) show the prominent horizontal resolution dependence of the simulated rainfall diurnal cycle, based on the superior performance of 3.5 km run compared to 14 km and 7 km simulation using Global Cloud-Resolving Model. WRF simulation with the convection-permitting spatial resolution (2 km) also shows much better results of rainfall diurnal pattern than those with 50 km and 10 km resolution in western Java and southern Malay Peninsula (Argueso et al. 2017).

The evaluation of model performance in terms of the major characteristics of diurnal variation of rainfall is important to evaluate the physical basis of model and also useful to understand the important mechanisms that drive rainfall processes. Different regional models show different performances (e.g., Koo and Hong 2010), but even the same regional model with different configurations show a significantly different performance (e.g., Huang et al. 2013). In this regard, it is necessary to optimize the model performance for a range of resolution settings and physics parameterizations.

[Acknowledgements]

This research is supported by the National Research Foundation Singapore under its Campus for Research Excellence and Technological Enterprise programme. The Center for Environmental Sensing and Modeling is an interdisciplinary research group of the Singapore MIT Alliance for Research and Technology. The first author was partly supported by the Korea Agency for Infrastructure Technology Advancement (KAIA) grant funded by the Ministry of Land, Infrastructure and Transport (Grant 17AWMP-B083066-04).

References

Arakawa O, Kitoh A (2005) Rainfall diurnal variation over the Indonesian Maritime Continent simulated by 20 km mesh GCM. SOLA 1:109-112

Argueso D, Di Luca A, Evans JP (2016) Precipitation over urban area in the western Maritime Continent using a convection-permitting model. Clim Dyn 47: 1143-1159.

Birch C, Roberts M, Garcia-Carreras L, Ackerley D, Reeder M, Lock A, Schiemann R (2015) Sea breeze dynamics and convection initiation: the influence of convective parameterization in weather and climate model biases. J Clim. doi: http://dx.doi.org/10.1175/JCLI-D-14-00850.1

Da Rocha RP, Morales CA, Cuadra SV, Ambrizzi T (2009) Precipitation diurnal cycle and summer climatology assessment. J Geophys Res 114: D10108. Doi:10.1029/2008JD010212

Dai A, Giorgi F, Trenberth KE (1999) Observed and model-simulated diurnal cycles of precipitation over the contiguous United States. J Geophys Res 104: 6377-6402

Evans JP, Westra S (2012) Investigating the mechanisms of diurnal rainfall variability using a regional climate model. J Clim 25:7232-7247

Gianotti RL (2012) Convective cloud and rainfall processes over the Maritime Continent: Simulation and analysis of the diurnal cycle. Ph.D. dissertation, Massachusetts Institute of Technology, 306 pp.

Gianotti RL, Eltahir EAB (2014) Regional climate modeling over the Maritime Continent. Part I: New parameterization for convective cloud fraction. J Clim 27:1488-1503

Gianotti RL, Eltahir EAB (2014) Regional climate modeling over the Maritime Continent. Part II: New parameterization for autoconversion of convective rainfall. J Clim 27:1504-1523

Gianotti RL, Zhang D., Elfatih EAB (2012) Assessment of the Regional Climate Model Version 3 over the Maritime Continent using different cumulus parameterization and land use schemes. J. Clim 25:638-656

Huang WR, Chan JCL (2011) Maintenance mechanisms for the early-morning maximum summer rainfall over southeast China. Q J R Meteorol Soc 137:959-968

Huang WR, Chan JCL, Au-Yeung AYM (2013) Regional climate simulations of summer diurnal rainfall variations over East Asia and Southeast China. Clim Dyn 40:1625-1642

Huffman GJ et al (2007) The TRMM Multisatellite Precipitation Analysis (TMPA): Quasi-Global, Multiyear, Combined-Sensor Precipitation Estimates at Fine Scales. J Hydrometeorol 8:38-55.

Ichikawa H, Yasunari T (2006) Time-Space characteristics of diurnal rainfall over Borneo and surrounding oceans as observed by TRMM-PR. J Clim 19:1238-1260

Ichikawa H, Yasunari T (2008) Intraseasonal variability in diurnal rainfall over New Guinea and the surrounding oceans during Austral Summer. J Clim 21:2852-2868

Im ES, Gianotti RL, Eltahir EAB (2014) Improving the simulation of the West African Monsoon using the MIT regional Climate Model. J Clim 27:2209-2229

Kikuchi K, Wang B (2008) Diurnal precipitation regimes in the global tropics. J Clim 21:2680-2696

Koo MS, Hong SY (2010) Diurnal variations of simulated precipitation over East Asia in two regional climate models. J Geophys Res 115: D05105. doi:10.1029/2009JD012574.

Lee MI et al (2007) Sensitivity to horizontal resolution in the AGCM simulations of warm season diurnal cycle of precipitation over the United Sates and Northern Mexico. J Clim 20:1862-1881

Lee MI et al (2008) Role of convection triggers in the simulation of the diurnal cycle of precipitation over the United States Great Plains in a general circulation model. J Geophys Res 113: D02111. doi:10.1029/2007JD008984.

Leung LR, Qian Y (2003) The sensitivity of precipitation and snowpack simulations to model resolution via nesting in regions of complex terrain. J Hydrometeorol 4:2015-1043

Liu X, Bai A, Liu C (2009) Diurnal variations of summertime precipitation over the Tibetan Plateau in relation to orographically-induced regional circulations. Environ Res Lett 4:045203

Love BS, Matthews AJ, Lister GMS (2011) The diurnal cycle of precipitation over the Maritime Continent in a high-resolution atmospheric model. Q J R Meteorol Soc 137: 934-947

Marcella MP (2012) Biosphere-Atmosphere Interactions over Semi-arid Regions: Modeling the Role of Mineral Aerosols and Irrigation in the Regional Climate System. Ph.D. dissertation, Massachusetts Institute of Technology, 282 pp.

Mori S et al (2004) Diurnal land-sea rainfall peak migration over Sumatera Island, Indonesian Maritime Continent, observed by TRMM satellite and intensive rawinsonde soundings. Mon Wea Rew 132:2021-2039

Oh JH, Kim KY, Lim GH (2012) Impact of MJO on the diurnal cycle of rainfall over the western Maritime Continent in the austral summer. Clim Dyn 38:1167-1180

Oki T, Musiake K (1994) Seasonal change of the diurnal cycle of precipitation over Japan and Malaysia. J Appl Meteorol 33:1445-1463

Pal JS et al (2007) The ICTP RegCM3 and RegCNET: regional climate modeling for the developing world. Bull Am Meteorol Soc 88:1395-1409

Ploshay J, Lau NC (2010) Simulation of the diurnal cycle in tropical rainfall and circulation during boreal summer with a high-resolution GCM. Mon Wea Rew 138:3434-3452

Pribadi A, Wongwises P, Humphries U, Limsakul A, Wangwongchai A (2012) Diurnal rainfall variation over three regions within Indonesia based on Ten Years of TRMM data. J Sustainable Energy & Environment 3:81-86

Pritchard MS, Somerville RCJ (2009) Empirical orthogonal function analysis of the diurnal cycle of precipitation in a multi-scale climate model. Geophys Res Lett 36: L05812. doi:10.1029/2008GL036964.

Qian JH (2008) Why precipitation is mostly concentrated over islands in the Maritime Continent. J Atmos Sci 65:1428-1440

Reboita MS, Dutra LMM, Dias CG (2016) Diurnal cycle of precipitation simulated by RegCM4 over South America: present and future scenarios. Clim Res 70:39-55. Doi:10.3354/cr01416

Sato T, Miura H, Satoh M, Takayabu YN, Wang Y (2009) Diurnal cycle of precipitation in the tropics simulated in a global cloud-resolving model. J Clim 21:4809-4826

Sato T, Yoshikane T, Satoh M, Miura H, Fujinami H (2008) Resolution dependency of the diurnal cycle of convective clouds over the Tibetan Plateau in a mesoscale model. J Meteor Soc Japan 86A: 17-31

Schiemann R, Demory ME, Mizielinski MS, Roberts MJ, Shaffrey LC, Strachan J, Vidale PL (2014) The sensitivity of the tropical circulation and Maritime Continent precipitation to climate model resolution. Clim Dyn 42:2455-2468

Takayabu YN, Kimoto M (2008) Diurnal march of rainfall simulated in a T106 AGCM and dependence on cumulus schemes. J Meteor Soc Japan 86A:163-173

Teo CK, Koh TY, Lo JCF, Bhatt BH (2011) Principal component analysis of observed and modeled diurnal rainfall in the Maritime Continent. J Clim 24:4662-4675

Uppala S, Dee D, Kobayashi S, Berrisford P, Simmons A (2008) Towards a climate data assimilation system: status update of ERAInterim. ECMWF Newsletter 115:12-18

Wang Y, Zhou L, Hamilton K (2007) Effect of convective entrainment/detrainment on the simulation of the tropical precipitation diurnal cycle. Mon Wea Rew 135:567-585

Winter JM, Pal JS, Eltahir EAB (2009) Coupling of Integrated Biosphere Simulator to Regional Climate Model Version 3. J Clim 22:2743-2756

Wu P, Hara M, Hamada JI, Yamanaka MD, Kimura F (2009) Why a large amount of rain falls over the Sea in the Vicinity of Western Sumatra Island during Nighttime. J Appl Meteor Climatol 48: 1345-1361.

Wu P, Yamanaka MD, Matsumoto J (2008) The formation of nocturnal rainfall offshore from convection over Western Kalimantan (Borneo) island. J Meteor Soc Japan 86A:187-203

Xu Y, Zhang Y, Lin E, Lin W, Dong W, Jones R, Hassell D, Wilson S (2006) Analyses on the climate change responses over China under SRES B2 scenarios using PRECIS. Chinese Science Bulletin 51:2260-2267. Doi:10.1007/s11434-006-2099-8

Zhou L, Wang Y (2006) Tropical Rainfall Measuring Mission observation and regional model study of precipitation diurnal cycle in the New Guinean region. J Geophys Res 111:D17104. doi:10.1029/2006JD007243.

Table and Figure Captions

Table 1. Cloud liquid water content (g m^{-3}) used to calculate new convective cloud fraction.

Table 2. Area-averaged annual and seasonal (DJF and JJA) mean rainfall derived MRCM27 and MRCM12 simulations and TRMM observation (unit: mm/day).

Table 3. Fractional areas where the simulated peak timing in the diurnal variation corresponds exactly to the one from TRMM observation (0 Hour) and is delayed or advanced within 3hour compared to the one from TRMM observation (±3 Hour).

FIG. 1. Topography (unit: m) used for (a) 27 km and (b) 12 km simulations using MRCM over the Maritime Continent. Blue dotted lines are the location for the analysis along the west-east transects (Latitude:3°S) to examine the rainfall characteristics (see Fig. 8) and along the south-north transects (Longitude:102°E) to examine the vertical structure of circulation (see Fig. 10).

FIG. 2. Spatial distribution of rainfall (unit: mm/day) averaged over DJF derived from the (a) MRCM27 and (b) MRCM12 simulation, and (c) TRMM observations, and (d-e) difference between simulation and observation.

FIG. 3. Latitude–time cross section of monthly mean rainfall (unit: mm/day) averaged from 95°E to 119°E from the (a) MRCM27 and (b) MRCM12 simulations, and (c) TRMM observations.

FIG. 4. Diurnal variations of rainfall rate (unit: mm/hour) averaged over land (denoted by _L) and ocean (denoted by _O) from the MRCM27 and MRCM12 simulations, and TRMM observation. Error bar indicates the interannual variation during 30-year. Red asterisk indicates that the difference between simulation and TRMM observation is significant at the 95% confidence level.

FIG. 5. Timing appeared in the maximum rainfall of the diurnal variation from the (a) MRCM27 and (b) MRCM12 simulations, and (c) TRMM observation. The red rectangular box indicates the area to enlarge for the examination of the propagation feature of diurnal variation shown in Fig. 6.

FIG. 6. Timing appeared in the maximum rainfall of the diurnal variation from the (a) MRCM27 and (b) MRCM12 simulations, and (c) TRMM observation. Dashed lines presented in (a) and (b) indicate the topography (unit: m) used for MRCM27 and MRCM12 simulations.

FIG. 7. Spatial distribution of the normalized amplitude of diurnal cycle (i.e. (maximum–minimum)/mean) from the (a) MRCM27 and (b) MRCM12 simulations, and (c) TRMM observation.

FIG. 8. Time-longitude cross section of (a, d, g) total, (b, e) convective, and (c, f) large-scale rainfall along the 3°S (horizontal dashed line in Fig. 1) derived from MRCM12 and MRCM27 simulations, and TRMM observation (only total rainfall).

FIG. 9. Anomalous wind (vector) and divergence (shading, 10^{-5} s^{-1}) at 12UTC (19LST) and 24UTC (07LST) derived from the MRCM27 and MRCM12 simulations.

FIG. 10. Vertical structure of omega (shading, 10^{-5} hPa s^{-1}) and meridional wind anomaly (contour, m s^{-1}) at 102°E from the MRCM27 and MRCM12 simulations.

Table 1. Cloud liquid water content (g m^{-3}) used to calculate new convective cloud fraction.

		MRCM	Reference value based on observation
Continental	Climatological cloud liquid water	1.0	0.1-3 from Rosenfeld and Lensky (1998)
	Threshold cloud water content	1.1	
Maritime	Climatological cloud liquid water	0.4	0.25-1.3 from Rangno and Hobbs (2005)
	Threshold cloud water content	0.45	

Table 2. Area-averaged annual and seasonal (DJF and JJA) mean rainfall derived MRCM27 and MRCM12 simulations and TRMM observation (unit: mm/day).

		MRCM27	MRCM12	TRMM
ANN	**Whole**	6.0	6.9	7.8
	Land	9.0	9.6	8.3
	Ocean	4.6	5.5	7.6
DJF	**Whole**	7.3	8.6	9.3
	Land	10.6	11.4	9.7
	Ocean	5.7	7.3	9.2
JJA	**Whole**	4.4	5.0	6.2
	Land	5.8	6.2	5.9
	Ocean	3.7	4.4	6.3

Table 3. Fractional areas where the simulated peak timing in the diurnal variation corresponds exactly to the one from TRMM observation (0 Hour) and is delayed or advanced within 3hour compared to the one from TRMM observation (±3 Hour).

	Whole		**Land**		**Ocean**	
	0 Hour	**0 Hour & ±3 Hour**	**0 Hour**	**0 Hour & ±3 Hour**	**0 Hour**	**0 Hour & ±3 Hour**
MRCM27	18.8%	61.7%	22.3%	77.8%	16.8%	52.8%
MRCM12	21.5%	62.6%	25.2%	80.8%	19.4%	52.6%

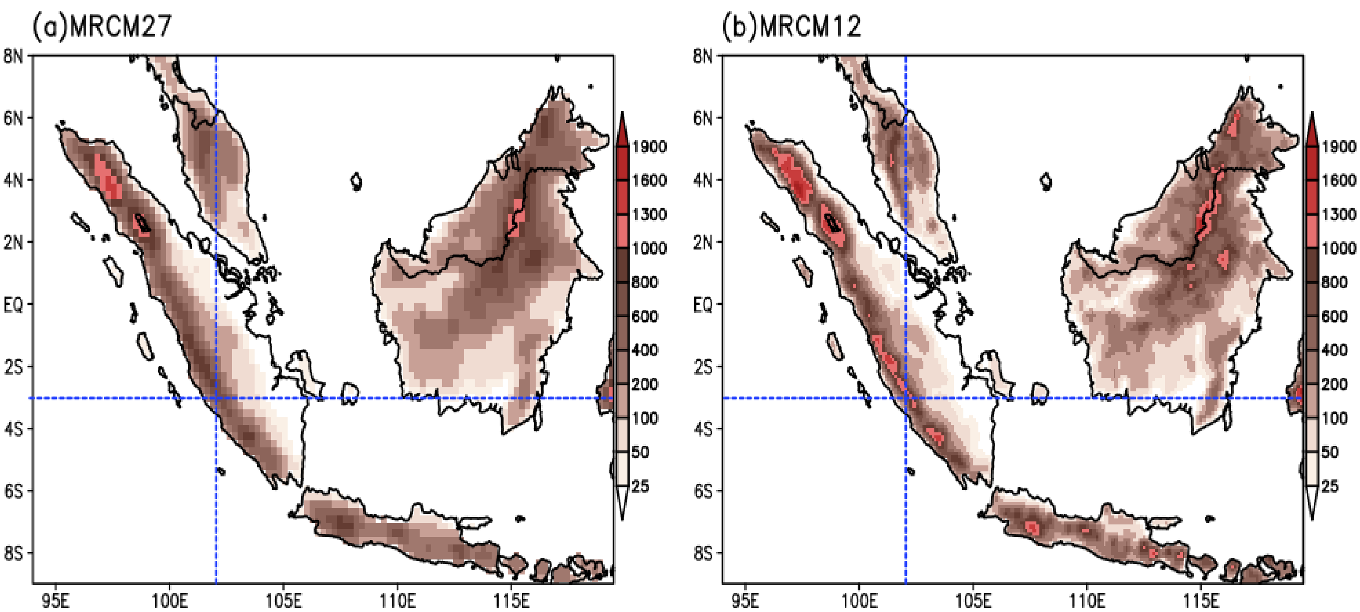

FIG. 1. Topography (unit: m) used for (a) 27 km and (b) 12 km simulations using MRCM over the Maritime Continent. Blue dotted lines are the location for the analysis along the west-east transects (Latitude:3°S) to examine the rainfall characteristics (see Fig. 8) and along the south-north transects (Longitude:102°E) to examine the vertical structure of circulation (see Fig. 10).

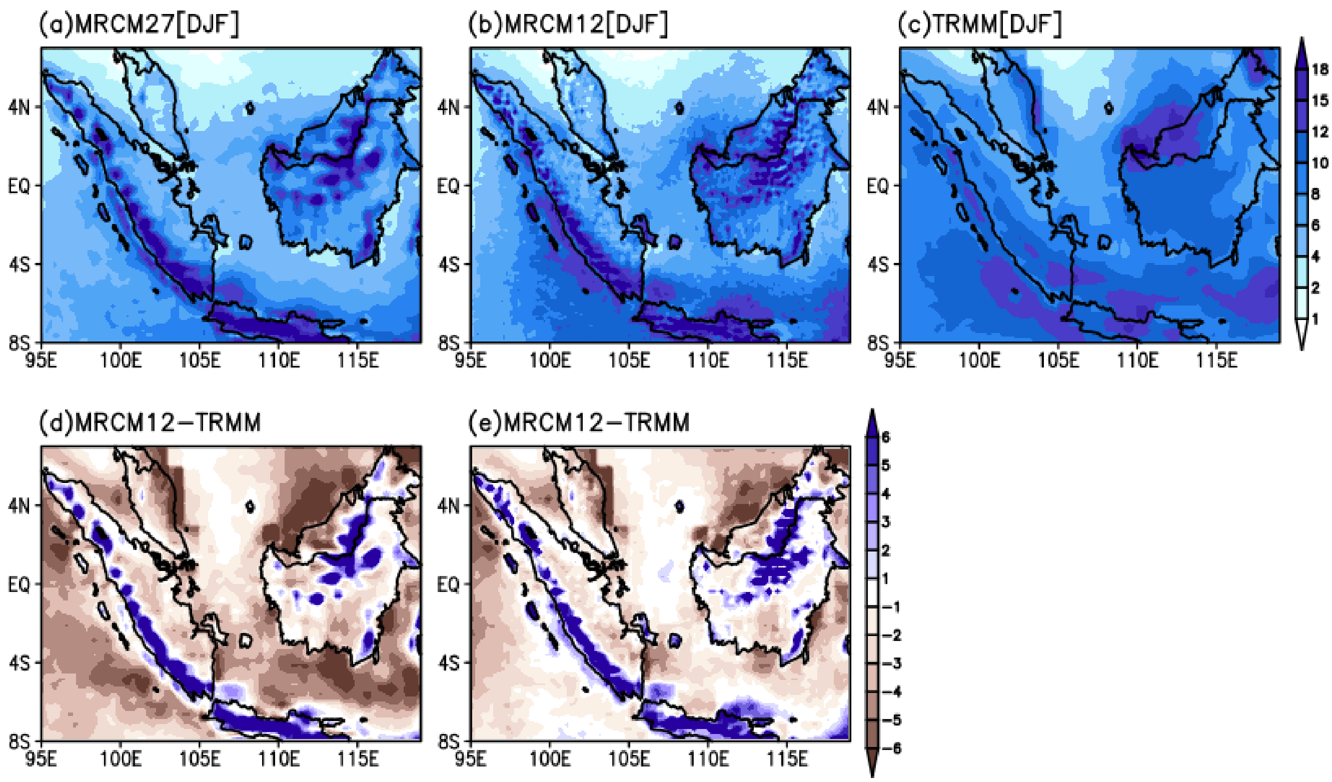

FIG. 2. Spatial distribution of rainfall (unit: mm/day) averaged over DJF derived from the (a) MRCM27 and (b) MRCM12 simulation, and (c) TRMM observations, and (d-e) difference between simulation and observation.

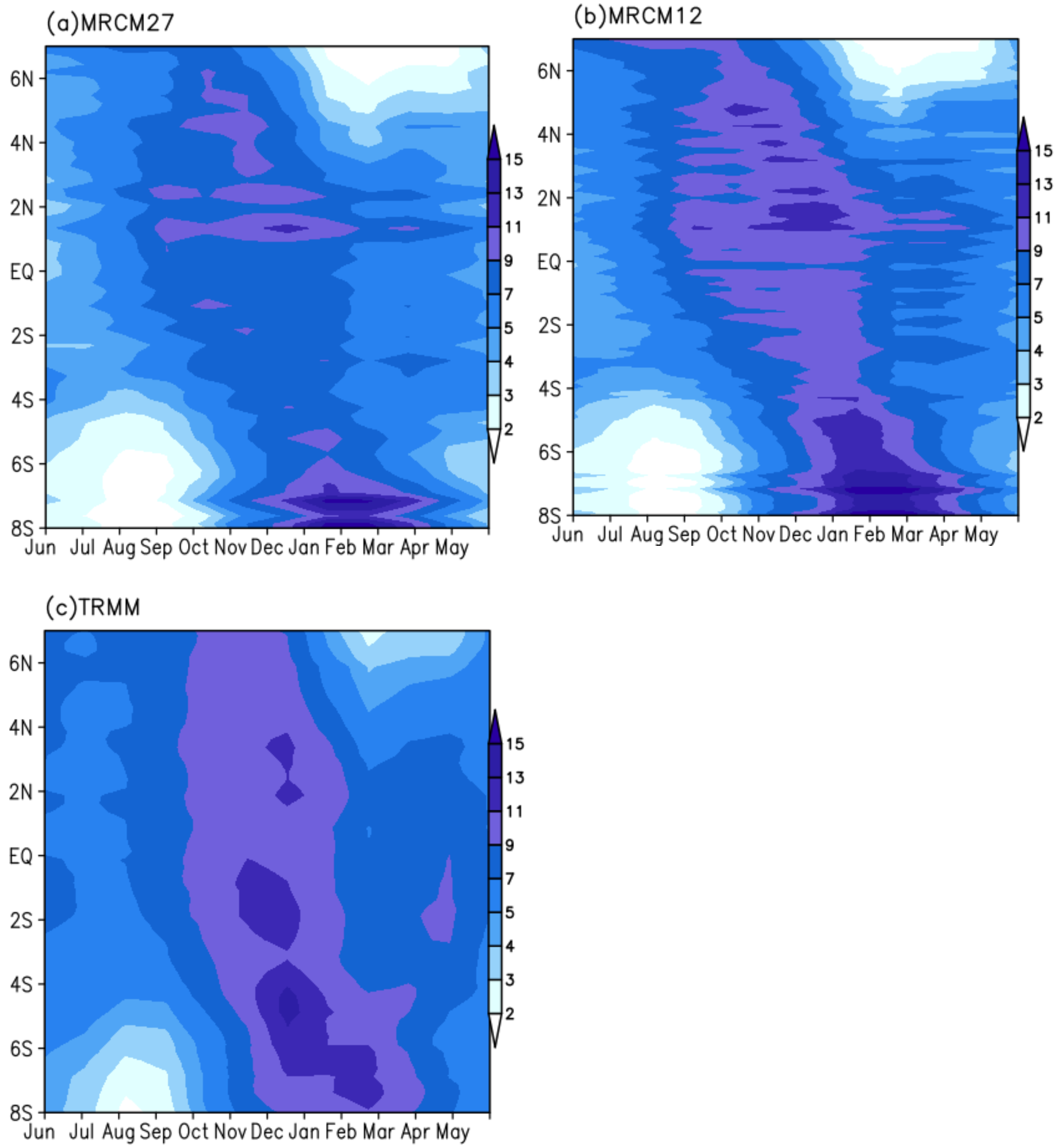

FIG. 3. Latitude–time cross section of monthly mean rainfall (unit: mm/day) averaged from 95°E to 119°E from the (a) MRCM27 and (b) MRCM12 simulations, and (c) TRMM observations.

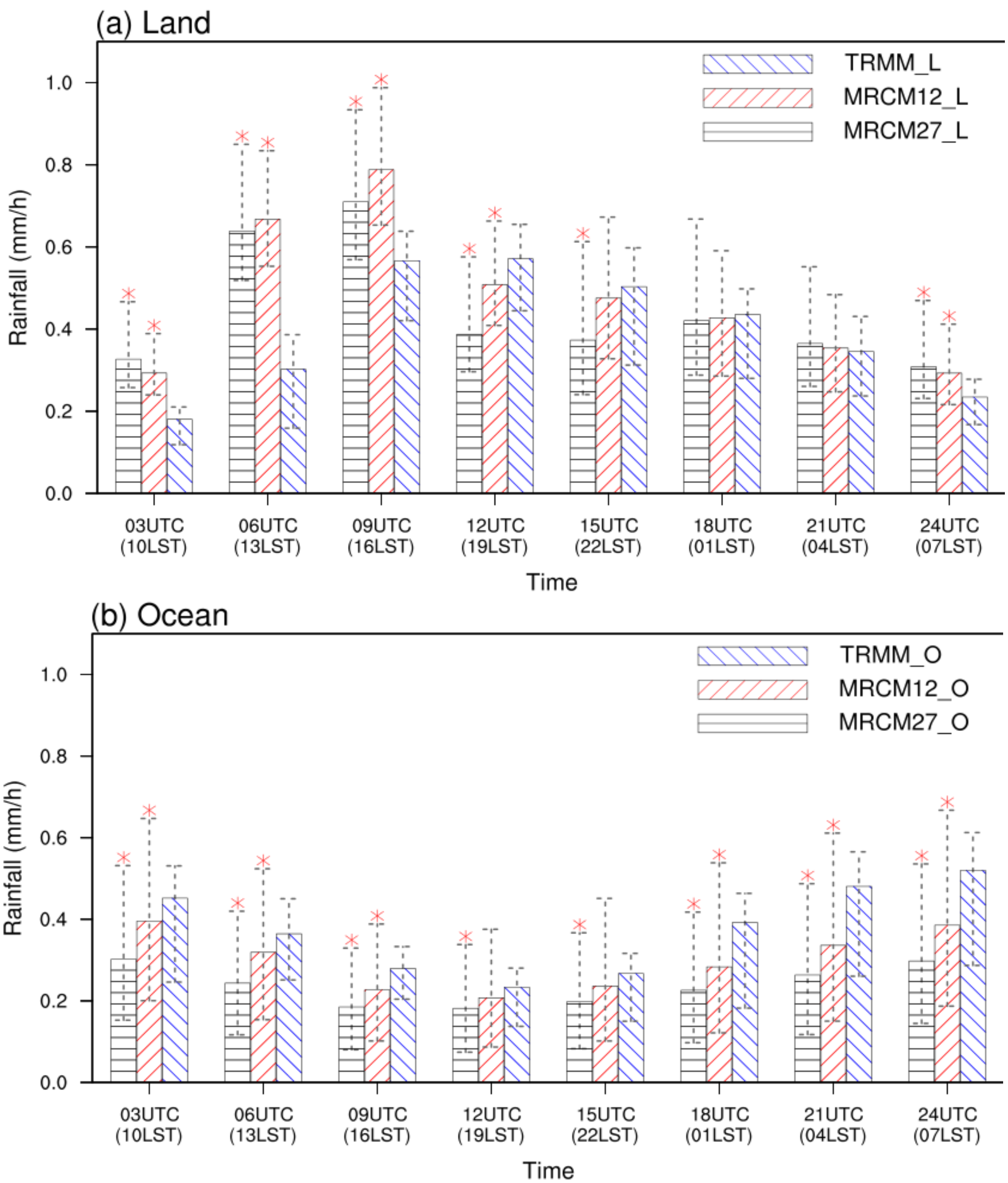

FIG. 4. Diurnal variations of rainfall rate (unit: mm/hour) averaged over land (denoted by _L) and ocean (denoted by _O) from the MRCM27 and MRCM12 simulations, and TRMM observation. Error bar indicates the interannual variation during the 30-year period. Red asterisk indicates that the difference between simulation and TRMM observation is significant at the 95% confidence level.

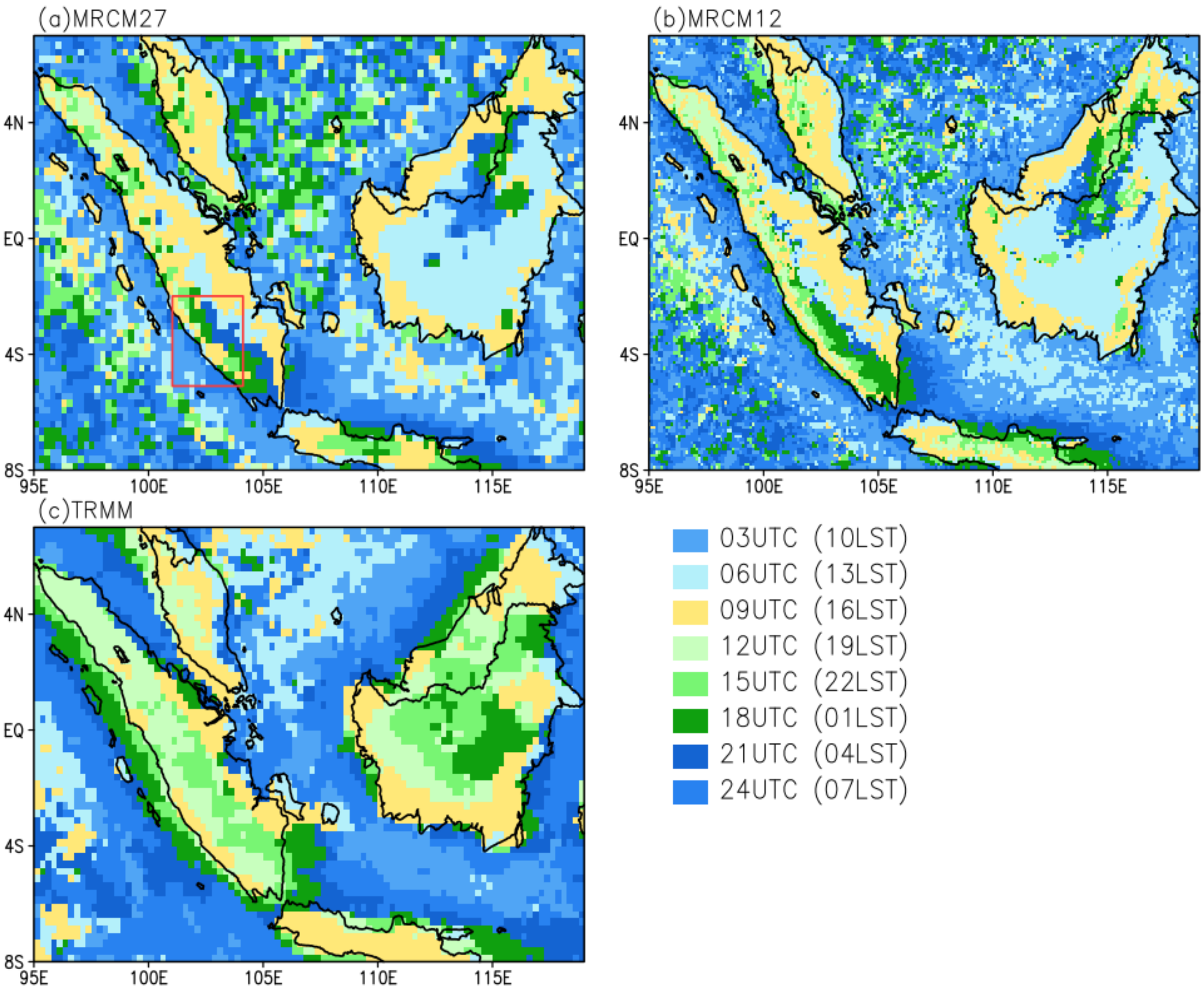

FIG. 5. Timing appeared in the maximum rainfall of the diurnal variation from the (a) MRCM27 and (b) MRCM12 simulations, and (c) TRMM observation. The red rectangular box indicates the area to enlarge for the examination of the propagation feature of diurnal variation shown in Fig. 6.

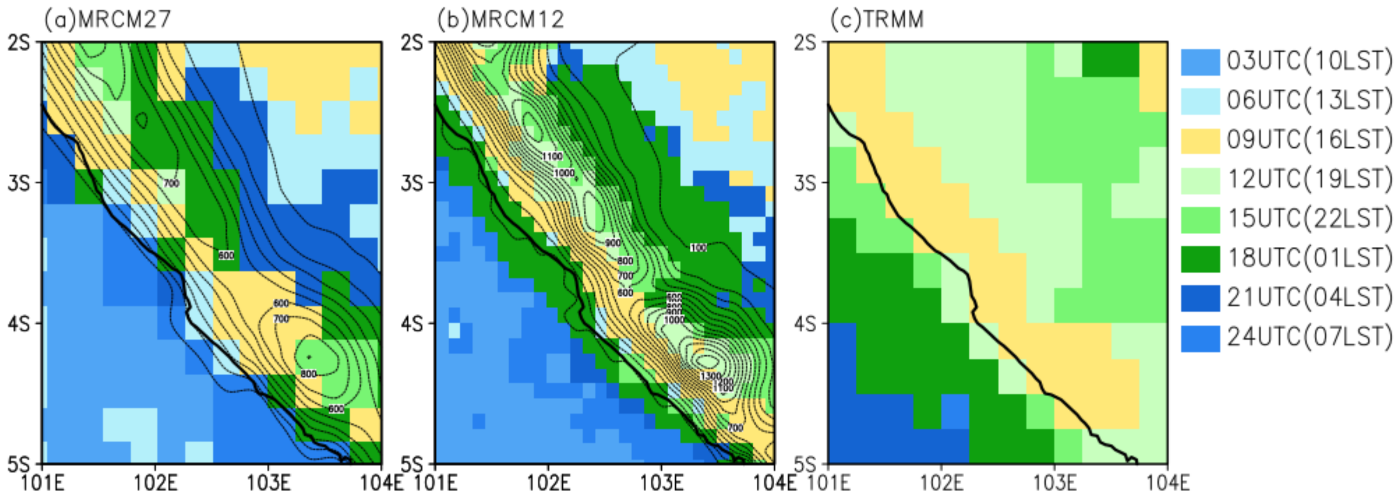

FIG. 6. Timing appeared in the maximum rainfall of the diurnal variation from the (a) MRCM27 and (b) MRCM12 simulations, and (c) TRMM observation. Dashed lines presented in (a) and (b) indicate the topography (unit: m) used for MRCM27 and MRCM12 simulations.

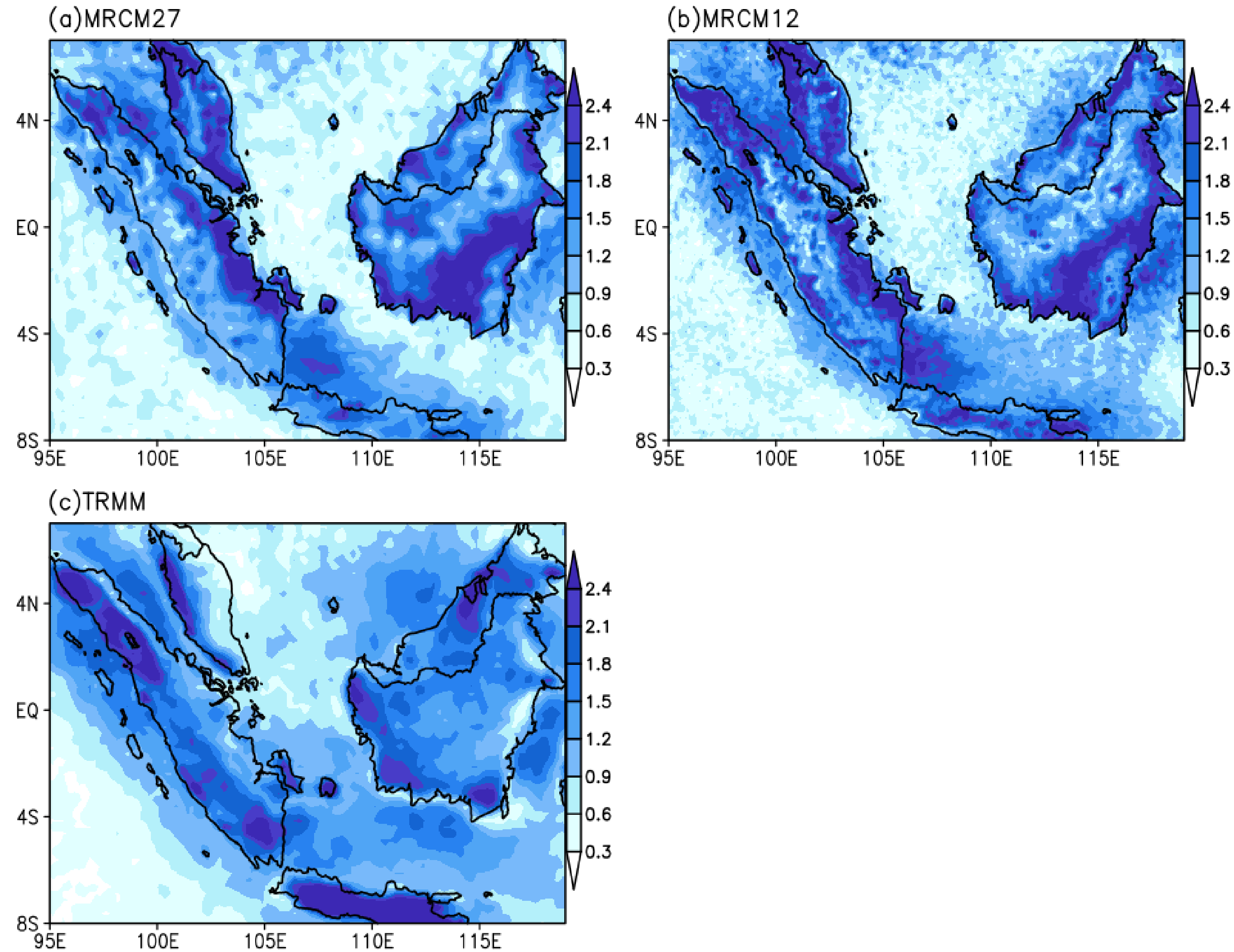

FIG. 7. Spatial distribution of the normalized amplitude of diurnal cycle (i.e. (maximum–minimum)/mean) from the (a) MRCM27 and (b) MRCM12 simulations, and (c) TRMM observation.

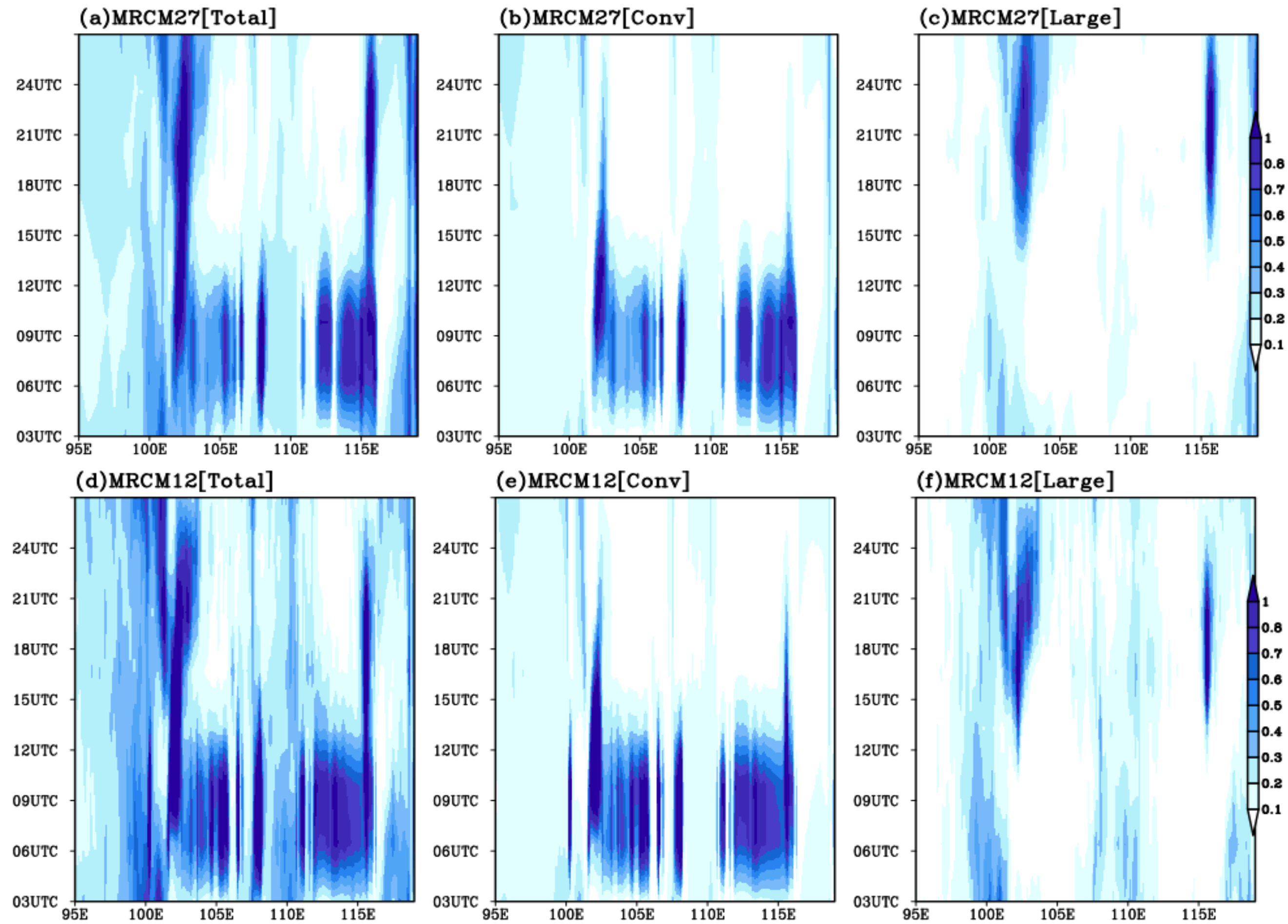

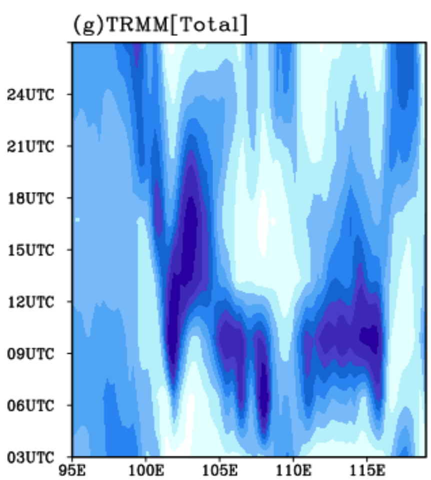

FIG. 8. Time-longitude cross section of (a, d, g) total, (b, e) convective, and (c, f) large-scale rainfall along the 3°S (horizontal dashed line in Fig. 1) derived from MRCM12 and MRCM27 simulations, and TRMM observation (only total rainfall).

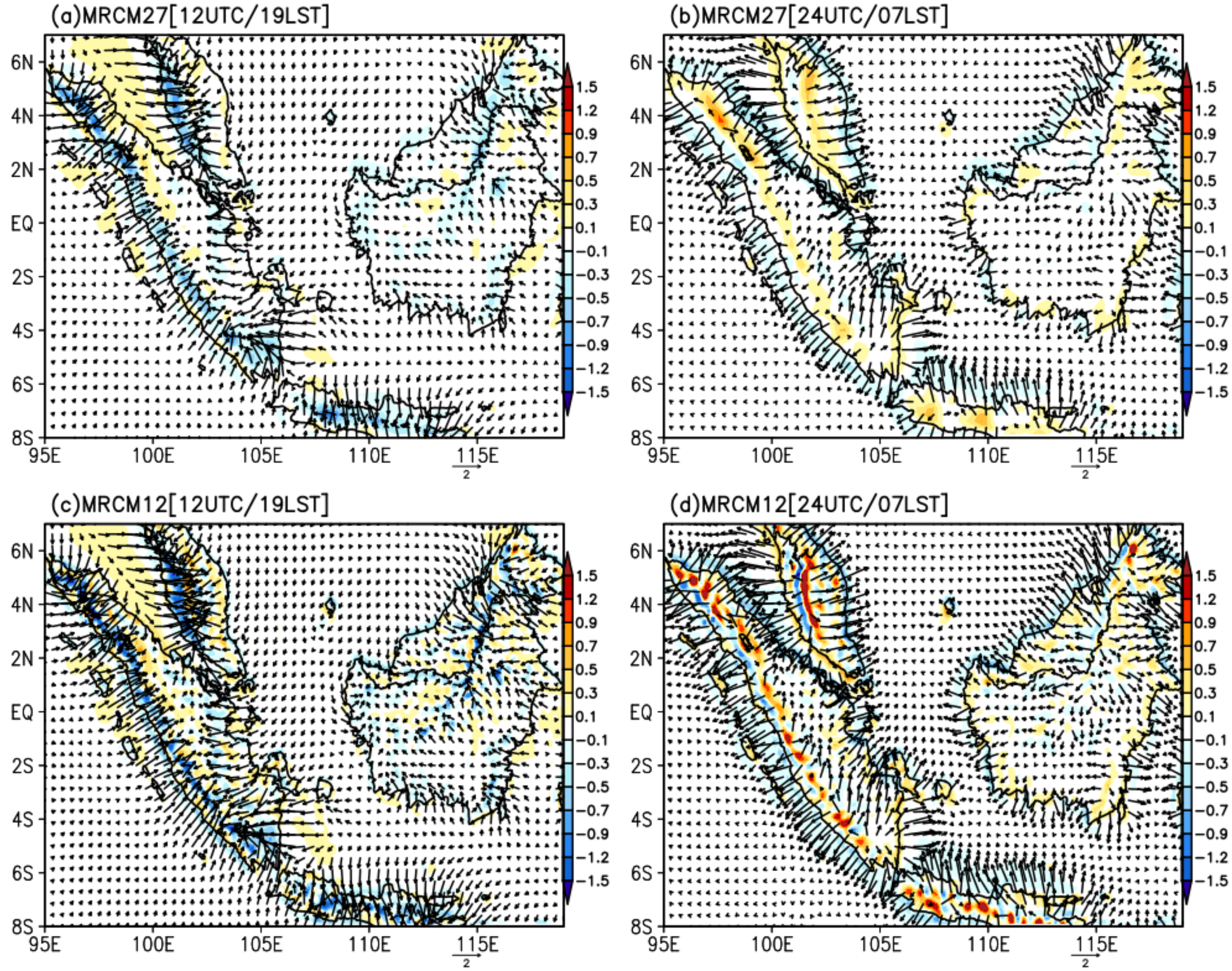

FIG. 9. Anomalous wind (vector) and divergence (shading, 10^{-5} s^{-1}) at 12UTC (19LST) and 24UTC (07LST) derived from the MRCM27 and MRCM12 simulations.

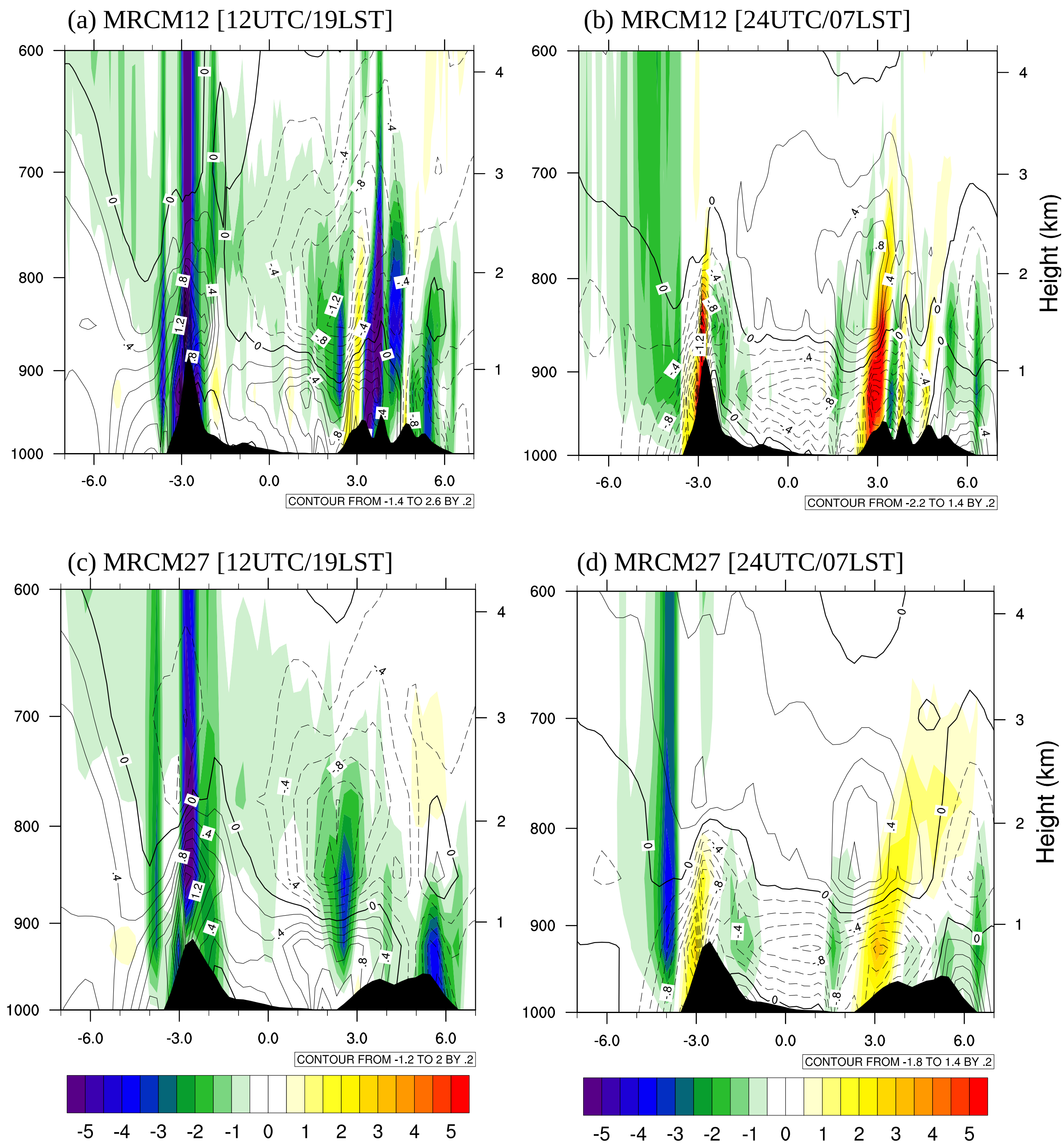

FIG. 10. Vertical structure of omega (shading, 10^{-5} hPa s^{-1}) and meridional wind anomaly (contour, m s^{-1}) at 102°E from the MRCM27 and MRCM12 simulations.